12 Superconductivity and Magnetism

M. Bendele, S. Bosma, Z. Guguchia, A. Ichsanov (till September 2010), H. Keller, A. Maisuradze (since April 2010), F. Murányi (till September 2010), J. Roos (till April 2010), S. Siegrist (since January 2010), E. Stilp (since December 2010), S. Strässle (till August 2010), S. Weyeneth, B. M. Wojek (till January 2011)

Visiting scientists: D. Di Castro, M.V. Eremin, B. Graneli, B.I. Kochelaev, R. Puzniak, A. Shengelaya

Emeritus members: K.A. Müller (Honorarprofessor), T. Schneider (Titularprofessor), M. Mali, J. Roos

in collaboration with:
ETH Zürich (J. Karpinski), Paul Scherrer Institute (K. Conder, R. Khasanov, E. Morenzoni), Max-Planck-Institute for Solid State Research Stuttgart (A. Bussmann-Holder), University of Geneva (Ø. Fischer, J. M. Triscone), University of Rome (D. Di Castro), Kazan State University (A. Dooglav, M. V. Eremin, B. I. Kochelaev), Polish Academy of Sciences (R. Puzniak), Tbilisi State University (A. Shengelaya).

We report on research projects in the field of high-temperature superconductors (HTS's) and materials with novel electronic properties. Our studies involve various complementary techniques, such as muon-spin rotation (μSR), electron paramagnetic resonance (EPR), nuclear magnetic resonance (NMR), nuclear quadrupole resonance (NQR), and SQUID and torque magnetometry. Besides focusing on cuprates and conventional superconductors, the investigations have been extended to the recently discovered iron-based superconductors.

12.1 Search for orbital currents in superconducting $YBa_2Cu_4O_8$

The concept of orbital currents (OC's) was proposed to explain the pseudogap of the cuprate superconductors [1]. However, the present state of knowledge about OC's is contradictory both in theory and experiment. No evidence for local fields was found i.e. in a yttrium nuclear magnetic resonance (NMR) investigation by our group [2].

Recently, Zeeman perturbed nuclear quadrupole resonance was applied to evaluate weak magnetic fields in the context of OC's in cuprate superconductors [3]. The magnetic environment of the barium atom in c-axis oriented powder samples of $YBa_2Cu_4O_8$ was investigated in the pseudogap phase at 90 K. The Ba atom is of particular interest since it is situated outside, but close to the copper oxide bilayer, at a position where the combined fields from the two neighboring layers would be enhanced because of the suggested ferromagnetic order within the bilayer. Zeeman perturbed nuclear resonance makes use of the fact that the Ba atom has both a quadrupolar and a nuclear magnetic moment. This technique is a rarely implemented variant of nuclear quadrupole resonance (NQR), which utilizes the local electric field gradient to lift the nuclear spin degeneracy. The Zeeman perturbation is introduced by means of an external coil as a weak static magnetic field (of order mT). For a typical ^{137}Ba NQR resonance line of a few hundred kHz width (see inset of Fig. 12.1), the resonance line split caused by a field of the order of mT would not be directly observable. The principle of the measurement is to detect a weak local magnetic field through a beat oscillation superposed on the Gaussian shaped decay of the spin echo intensity, caused by homonuclear dipolar fields (Fig. 12.1). In order to demonstrate the sensitivity of the technique for weak local magnetic fields, the Ba nucleus was studied at 300 K, where no OC's are expected. The result of this measurement is presented in Fig. 12.1, revealing the expected dominating Gaussian decay of the spin echo intensity with pulse separation

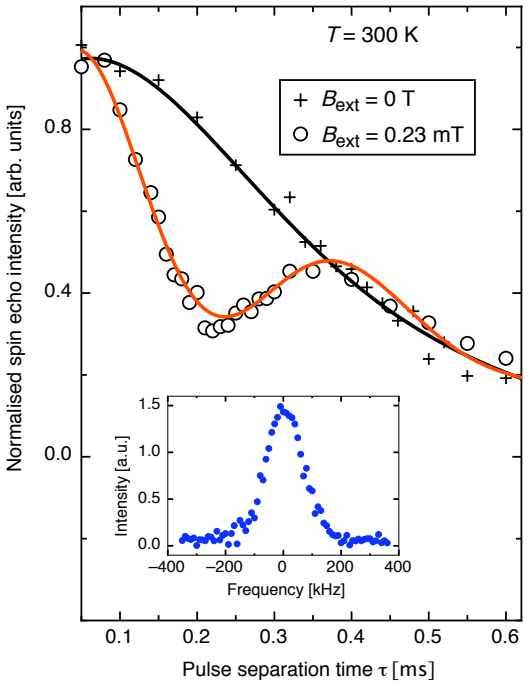

Fig. 12.1 – Dependence of the normalized ^{137}Ba spin-echo intensity as a function of the pulse separation time τ at 300 K for $B_{\rm ext}$ parallel to the c-axis of $YBa_2Cu_4O_8$. Results are shown for $B_{\rm ext}$ =0 T and $B_{\rm ext}$ =0.23 mT. The inset shows the ^{137}Ba resonance line at 300 K in zero external field.

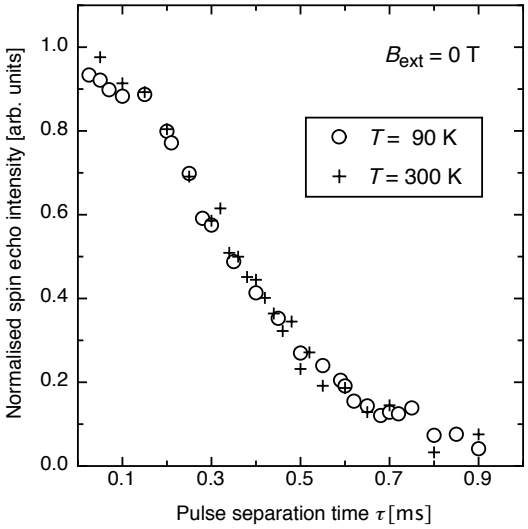

Fig. 12.2 – Spin echo intensity decay with pulse separation time τ in c-axis oriented $YBa_2Cu_4O_8$ for no applied field at 300 K and 90 K. No distinguishable difference in the normalized intensity was detected in the pseudogap phase.

time τ. This curve is our zero-field reference. The measurement procedure was calibrated using applied Zeeman fields of known strength. Fields calculated from the response were found to deviate less than 0.07 mT from the Zeeman fields actually applied with the calibrated external coil. In all experiments, background contributions, including Earth's magnetic field, were shielded.

In conclusion, the results, as evident from Fig. 12.2 do not indicate the presence of local fields at the Ba site in the pseudogap phase of c-axis oriented $YBa_2Cu_4O_8$. The detection limit of our method excludes static or dynamic field larger than 0.07 mT and 0.7 mT, respectively [3].

[1] S. Chakravarty *et al.*, Phys. Rev. B **63**, 094503 (2001).

[2] S. Strässle *et al.*, Phys. Rev. Lett. **101**, 237001 (2008).

[3] S. Strässle *et al.*, Phys. Rev. Lett. **106**, 097003 (2011).

12.2 Iron isotope effects in the iron-based superconductor $FeSe_{1-x}$

In 1990 we started a project on isotope effects in cuprate HTS's at the University of Zurich. Since then we performed a number of isotope effect studies. As a result, we observed several novel oxygen isotope ($^{16}O/^{18}O$) effects (OIE's) on different quantities in cuprate HTS's, including i.e. the transition temperature T_c, the in-plane magnetic penetration depth $\lambda_{ab}(0)$, the pseudogap temperature T^*, the superconducting energy gap Δ_0, the Néel temperature T_N, and the spin-glass freezing temperature T_g [1; 2]. All these unconventional OIE's clearly indicate that lattice effects are effective in all phases of cuprate HTS's imposing serious constraints on theoretical models [3].

Recently, we started an investigation of the Fe iso-

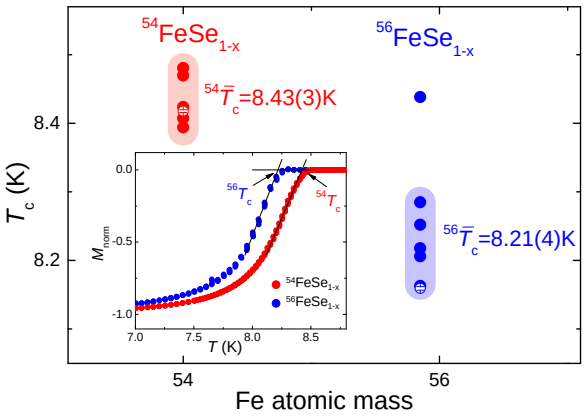

Fig. 12.3 – The superconducting transition temperature of $FeSe_{1-x}$ as a function of Fe atomic mass. The open symbols correspond to the samples studied by neutron powder diffraction. The inset shows the normalized magnetization curves for a pair of $^{54}FeSe_{1-x}$ and $^{56}FeSe_{1-x}$ samples.

tope effect (FeIE) on T_c in the iron-based superconductor $FeSe_{1-x}$ belonging to the "11" family [4]. The substitution of natural Fe (containing $\simeq$ 92% of ^{56}Fe) by its lighter isotope ^{54}Fe in $FeSe_{0.975}$ ($T_c \simeq 8.2$ K) leads an isotope shift of the transition temperature of $\Delta T_c = 0.22(5)$ K, corresponding to an FeIE exponent $\alpha_{Fe} = 0.81(15)$ (see Fig. 12.3) [4].

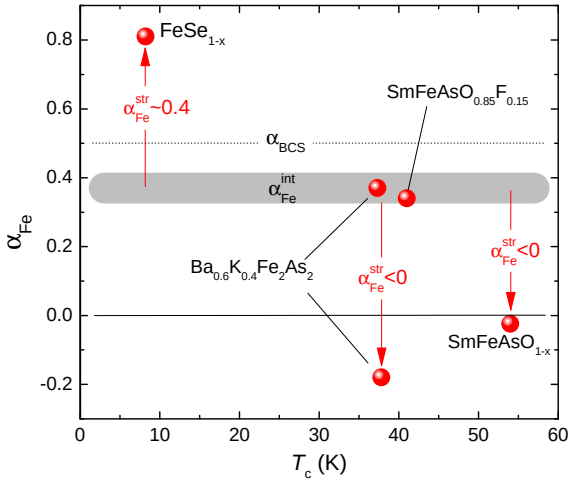

Fig. 12.4 – Fe isotope exponent α_{Fe} versus superconducting transition temperature ($FeSe_{1-x}$ [4], $Ba_{0.6}K_{0.4}Fe_2As_2$ and $SmFeAsO_{0.85}F_{0.15}$ [6], $Ba_{0.6}K_{0.4}Fe_2As_2$ [7], and $SmFeAsO_{1-x}$ [8]). The arrows indicate the direction of the shift from the intrinsic FeIE exponent $\alpha^{int}_{Fe} \simeq 0.35$ to 0.4 caused by structural effects.

This value is positive and considerably larger than the BCS value $\alpha_{BCS} = 0.5$.

In addition, the lattice parameters of the ^{54}Fe /^{56}Fe exchanged $FeSe_{1-x}$ samples were investigated carefully by neutron powder diffraction. It turned out that the a- and b-axes are slightly larger for $^{54}FeSe_{1-x}$ than those for $^{56}FeSe_{1-x}$, while the c-axis is marginally smaller for $^{54}FeSe_{1-x}$ than for $^{56}FeSe_{1-x}$. However, the volume of the unit cell remains unchanged. These slight differences in the lattice constants in the Fe isotope exchanged samples give rise to a slight change of the shape of the Fe_4Se pyramid and anion height which is known to affect T_c in Fe-based HTS's [5], and in turn may contribute to the total Fe isotope shift of T_c [4].

The currently reported results of the FeIE on T_c in Fe-based HTS's are highly controversial. The values of the FeIE exponent α_{Fe} for various families of Fe-based HTS were found to be as well positive ($\alpha_{Fe} \simeq 0.3$ to 0.4) [6], as negative ($\alpha_{Fe} \simeq$ -0.18 to -0.02)) [7; 8], or even to be exceedingly larger than the BCS value $\alpha_{BCS} = 0.5$ as found for $FeSe_{1-x}$ ($\alpha_{Fe} \simeq 0.8$) [4]. Recently, we have shown [9] that the Fe isotope substitution causes small structural modifications which, in turn, affect T_c. Upon correcting the isotope effect exponent for these structural effects, an almost unique value of $\alpha_{Fe} \simeq 0.35$ to 0.4 is found for at least three different families of Fe-based HTS (see Fig. 12.4).

[1] G. M. Zhao *et al.*, J. Phys.: Condens. Matter **13**, R569 (2001).

[2] H. Keller, in *Superconductivity in Complex Systems*, edited by K. A. Müller and A. Bussmann-Holder, Structure and Bonding 114, Springer-Verlag, Berlin, Heidelberg, New York (2005) pp. 114-143.

[3] H. Keller, A. Bussmann-Holder, and K. A. Müller, Materials Today **11**, 38 (2008).

[4] R. Khasanov *et al.*, New J. Phys., **12**, 073024 (2010).

[5] Y. Mizuguchi *et al.*,
Supercond. Sci. Technol. **23**, 054013 (2010).
[6] R. H. Liu *et al.*,
Nature (London) **459**, 64 (2009).
[7] P. M. Shirage *et al.*,
Phys. Rev. Lett. **103**, 257003 (2009).
[8] P. M. Shirage *et al.*,
Phys. Rev. Lett. **105**, 037004 (2010).
[9] R. Khasanov *et al.*,
Phys. Rev. B **82**, 212505 (2010).

12.3 NMR study of the iron-pnictide system $EuFe_{1.9}Co_{0.1}As_2$

Among the iron-based pnictide HTS's, the family $EuFe_{2-x}Co_xAs_2$ is particularly interesting since Eu^{2+} is a rare-earth ion with a $4f^7$ electronic configuration and a total electron spin S=7/2. This compound is built up by $[FeAs]^{2-}$ layers, separated by layers of magnetic Eu^{2+} ions [1]. $EuFe_2As_2$ exhibits both a spin density wave (SDW) ordering of the Fe moments and an antiferromagnetic ordering of the localized Eu^{2+} moments below 190 K and 19 K, respectively [1; 2]. In contrast to the other '122' systems, where the substitution of Fe by Co leads to superconductivity [3], the compounds containing Eu^{2+} exhibit the onset of a superconducting transition but seem to be hindered to reach zero resistivity at ambient pressure [4]. The study of the interaction between the localized Eu^{2+} moments and the conducting Fe_2As_2 layer is important for the understanding of superconductivity. The conduction electrons essentially determine the unusual superconducting properties and the high T_c's.

In order to investigate the coupling between the Eu and $Fe_{1.9}Co_{0.1}As_2$ layers as well as to study the magnetic transitions in $EuFe_{1.9}Co_{0.1}As_2$, a combination of X-ray diffraction, magnetization, and ^{75}As nuclear magnetic resonance (NMR) experiments were performed on single crystals [5]. Magnetic susceptibility as well as ^{75}As-NMR measurements reveal a decrease of the SDW transition temperature to T_{SDW}=120 K for $EuFe_{1.9}Co_{0.1}As_2$.

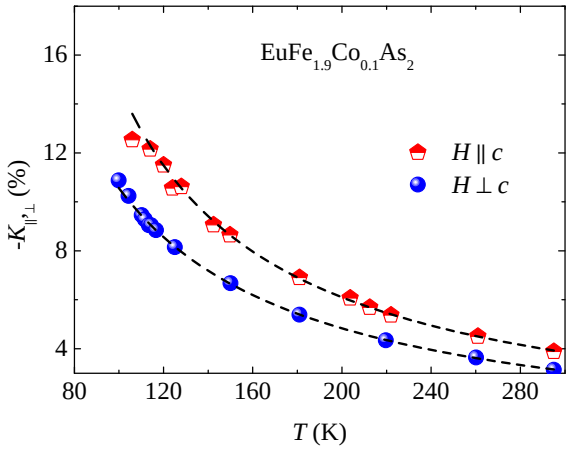

Fig. 12.5 – Temperature dependence of the ^{75}As magnetic shift in a single crystal $EuFe_{1.9}Co_{0.1}As_2$ for $H \parallel c$ and $H \perp c$. The dashed lines represent the Curie-Weiss behavior.

It was found that the ^{75}As NMR spectra are characterized by a large negative frequency shift with respect to the ^{75}As NMR Larmor frequency for all orientations of the magnetic field with respect to the crystallographic c-axis. The temperature dependence of the ^{75}As magnetic shift K above T_{SDW}=120 K is well described by a Curie-Weiss-like behavior $K(T)=K_0+C_K/(T+\Theta)$ for both $H \parallel c$ ($K_\parallel$) and $H \perp c$ ($K_\perp$) (see Fig. 12.5). This suggests that the temperature dependent part $K_{Eu}(T)$ of the shift arises from the hyperfine coupling between the ^{75}As nuclei and the Eu^{2+} $4f$ moments. A linear relation between K_{Eu} and the susceptibility χ_{Eu} of the localized Eu^{2+} $4f$ moments was observed, from which the hyperfine coupling constant A_{Eu} = -1.9×10^7 A/m per μ_B was estimated. This value of A_{Eu} is almost 60 times larger than the one reported for the '1111' system [6]. Such a large A_{Eu} indicates a strong coupling between the Eu^{2+} localized moments and the $Fe_{1.9}Co_{0.1}As_2$ layers, suggesting that the magnetic exchange interaction between the localized Eu $4f$ moments is mediated by the itinerant Fe $3d$ electrons. The strong interaction between the localized Eu^{2+} moments and the charge carriers in the $Fe_{2-x}Co_xAs_2$ layers may cause pair breaking [7], which may be the reason why it is difficult to reach superconductivity in $EuFe_{2-x}Co_xAs_2$.

[1] H. Raffius *et al.*, J. Phys. Chem. Solids **54**, 135 (1993).

[2] Y. Xiao *et al.*, Phys. Rev. B **80**, 174424 (2009).

[3] A. S. Sefat *et al.*, Phys. Rev. Lett. **101**, 117004 (2008).

[4] Y. He *et al.*, J. Phys.: Condens. Matter **22**, 235701 (2010).

[5] Z. Guguchia *et al.*, Phys. Rev. B, **83**, 144516 (2011).

[6] P. Jeglič *et al.*, Phys. Rev. B **79**, 094515 (2009).

[7] A. A. Abrikosov *et al.*, Zh. Eksp. Teor. Fiz. **39**, 1781 (1960).

12.4 Pressure effect on superconducting properties of $YBa_2Cu_3O_x$

$YBa_2Cu_3O_x$ was the first high temperature superconductor with a superconducting transition temperature T_c above the boiling point of nitrogen. However, the microscopic pairing mechanism leading to high-temperature superconductivity is still not resolved and is subject of intense debates. Hydrostatic pressure is a useful tool to tune the interatomic distances in the lattice which in turn modifies both the lattice dynamics [1] and the exchange coupling between Cu-spins in cuprates [2; 3]. Therefore, a detailed study of the pressure effect on superconducting properties, e.g. the superfluid density $\rho_s \propto 1/\lambda^2$, the gap magnitude Δ_0, and the BCS ratio, may provide important information to clarify the mechanism of superconductivity in the cuprates.

Recently, we performed muon-spin rotation (μSR) studies of the pressure effect on the magnetic penetration depth λ in $YBa_2Cu_3O_x$ at various oxygen concentrations ($6.45 \leqslant x \leqslant 6.98$). It is known that there are two contributions determining the pressure effect on T_c: (i) the charge transfer from the chain oxygen sites to the CuO_2 planes, and (ii) the pressure effect on the pairing interaction strength [4].

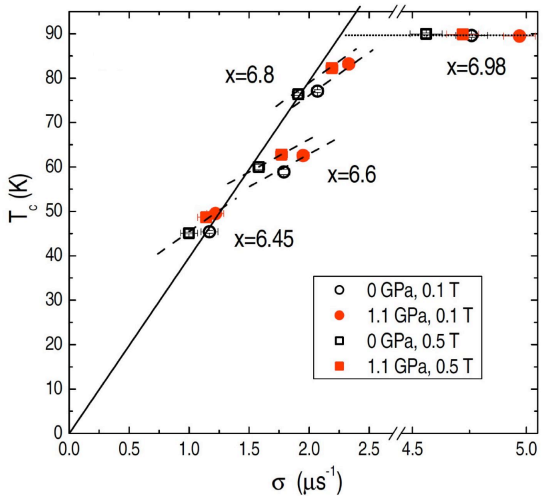

Fig. 12.6 – Uemura plot (T_c vs. σ) at zero and applied pressure $P = 1.1$ GPa for $YBa_2Cu_3O_x$ at various dopings x. The solid line is the Uemura line while the other lines are guides to the eye. The dashed lines show the pressure effect on the slope $\gamma = \partial\sigma/\partial T_c$ (see text).

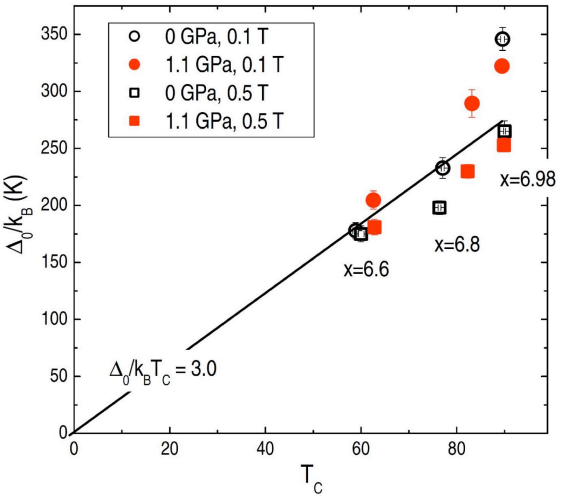

Fig. 12.7 – Relation of the zero-temperature gap Δ_0 and T_c in $YBa_2Cu_3O_x$ at different dopings, fields, and pressures. The solid line corresponds to $\Delta_0/k_B T_c = 3$.

While the first contribution at ambient pressure follows the Uemura relation [5], the second one, usually determined by the temperature dependence of thermodynamic properties under pressure, is not well studied so far. The μSR technique is a powerful tool to investigate the temperature dependence

of the superfluid density $\rho_s \propto \sigma \propto 1/\lambda^2$ at various pressures and fields. From the temperature dependence of the muon depolarization rate σ the value of $\sigma(T{=}0)$ and the gap-to-T_c (Δ_0/T_c) ratio were extracted (Figs. 12.6 and 12.7). Both quantities $\sigma(T{=}0)$ and Δ_0/T_c increase with increasing pressure P, implying that the coupling strength also increases with pressure. Interestingly, the Uemura relation [5] does not hold under pressure. The slope $\gamma = \partial T_c/\partial\sigma \simeq 20$ K/μs^{-1} is a factor of two smaller than that of the Uemura relation $\gamma_U = 40$ K/μs^{-1}. Note that the same slope was previously observed for the OIE on the magnetic penetration depth [6]. The parameter γ was found to be independent of the oxygen content for underdoped $YBa_2Cu_3O_x$ with an average value of $\gamma = 20(3)$ K/μs^{-1}. Taking into account the two mechanisms which increase T_c under pressure mentioned above, the two mechanisms also give rise to an increase of $\sigma = \sigma_U + \sigma_V$. While the first term accounts for the increase of the carrier concentration in the CuO_2 plane according to the Uemura relation, the second term is related to the modified pairing intercation V due to pressure.

Taking $\gamma = 20$ K/μs^{-1} for underdoped $YBa_2Cu_3O_x$ and using the previously reported value $\partial T_c/\partial P = 4$ K/GPa for underdoped $YBa_2Cu_3O_x$ [7], one may express the pressure effect on σ_V as follows: $\beta_P = \partial \ln \sigma_V/\partial P \equiv (\Delta\sigma_V/\sigma)/\Delta P \simeq 4\ /T_c$ GPa^{-1}. In this form the doping (or T_c) dependence of the pressure effect on σ_V resembles that of the OIE on σ: $\beta_M = \partial \ln \sigma/\partial \ln M$, where $\partial \ln M$ is the relative change of oxygen mass and $\partial P \propto \partial \ln M$. This implies that β_P is finite at optimal doping and increases with decreasing doping (or decreasing T_c). Additional studies should better clarify the relation between β_P and β_M.

In conclusion, both our studies of isotope effects in cuprates and iron-based superconductors and the recent studies on pressure effects on the magnetic penetration depth in doped $YBa_2Cu_3O_x$ strongly suggest that lattice effects are essential for the appearance of superconductivity in these systems.

[1] M. Calamiotou *et al.*, Phys. Rev. B **80**, 214517 (2009).

[2] W. A. Harrison, *Electronic Structure and the Properties of Solids* (Freeman, San Francisco, 1980).

[3] R. Ofer *et al.*, Phys. Rev. B **78**, 140508(R) (2008).

[4] X. J. Chen *et al.*, Phys. Rev. Lett. **85**, 2180 (2000).

[5] Y. J. Uemura *et al.*, Phys. Rev. Lett. **62**, 2317 (1989).

[6] H. Keller in *Superconductivity in complex systems*, ed. K. A. Müller and A. Bussmann-Holder, p. 114, Springer-Verlag Berlin, Heidelberg, New York (2005).

[7] C. C. Almasan *et al.* Phys. Rev. Lett. **69**, 680 (1992).